AIP Physics of Fluids

Large-eddy simulations of the turbulent Hartmann flow close to the transitional regime

I. E. Sarris, S. C. Kassinos, and D. Carati

Citation: Physics of Fluids (1994-present) **19**, 085109 (2007); doi: 10.1063/1.2757710
View online: http://dx.doi.org/10.1063/1.2757710
View Table of Contents: http://scitation.aip.org/content/aip/journal/pof2/19/8?ver=pdfcov
Published by the AIP Publishing

Articles you may be interested in

Constrained large-eddy simulation of laminar-turbulent transition in channel flow
Phys. Fluids **26**, 095103 (2014); 10.1063/1.4895589

Forced turbulence in large-eddy simulation of compressible magnetohydrodynamic turbulence
Phys. Plasmas **17**, 102307 (2010); 10.1063/1.3491835

A finite-volume variational multiscale method coupled with a discrete interpolation filter for large-eddy simulation of isotropic turbulence and fully developed channel flow
Phys. Fluids **18**, 115101 (2006); 10.1063/1.2391133

Large eddy simulation of magnetohydrodynamic turbulent channel flows with local subgrid-scale model based on coherent structures
Phys. Fluids **18**, 045107 (2006); 10.1063/1.2194967

Large-eddy simulation of high-Schmidt number mass transfer in a turbulent channel flow
Phys. Fluids **9**, 438 (1997); 10.1063/1.869138

Did your publisher get
18 MILLION DOWNLOADS in 2014?
AIP Publishing did.

AIP Publishing THERE'S POWER IN NUMBERS. Reach the world with AIP Publishing.

This article is copyrighted as indicated in the article. Reuse of AIP content is subject to the terms at: http://scitation.aip.org/termsconditions. Downloaded to IP: 195.130.98.66 On: Tue, 05 May 2015 19:49:17

Large-eddy simulations of the turbulent Hartmann flow close to the transitional regime

I. E. Sarris[a)]
Statistical and Plasma Physics, Université Libre de Bruxelles, Campus Plaine, 1050 Brussels, Belgium

S. C. Kassinos[b)]
Department of Mechanical and Manufacturing Engineering, University of Cyprus, CY-1678 Nicosia, Cyprus

D. Carati[c)]
Statistical and Plasma Physics, Université Libre de Bruxelles, Campus Plaine, 1050 Brussels, Belgium

(Received 15 January 2007; accepted 8 June 2007; published online 28 August 2007)

A series of large-eddy simulations (LES) of turbulent and transitional channel flows of a conductive fluid under the effect of a uniform magnetic field applied in the wall-normal direction, usually referred to as Hartmann flows, are performed using the dynamic Smagorinsky model. The flow is characterized by the hydrodynamic Reynolds number Re and the Hartmann number Ha that is related to the strength of the external magnetic field. Previous measurements and works on stability analysis have shown that a critical modified Reynolds number, based on the Hartmann layer thickness $R=\mathrm{Re}/\mathrm{Ha}$, exists at approximately $R=380$. Here, the LES are used to investigate the laminarization of flow when decreasing R. Also, similarities of the turbulent flows are explored for different values of Re and Ha but the same values of R or of the interaction parameter $N=\mathrm{Ha}^2/\mathrm{Re}$. The LES confirm that R is the relevant parameter that describes the transition and a critical Reynolds number for relaminarization is observed at $R\approx 500$. However, for turbulent flows at moderate values of the Ha and Re as considered in this study, the similarity with respect to N appears to be better than for R, especially for the first order statistics. Finally, the importance of the dynamic Smagorinsky model as the Hartmann number increases is discussed. © *2007 American Institute of Physics*. [DOI: 10.1063/1.2757710]

I. INTRODUCTION

Magnetohydrodynamic (MHD) turbulent flows are often encountered in engineering fields such as MHD pumps, crystal growth techniques, and conceptual designs of blankets of fusion reactors. For laboratory and industrial scale flows of conducting fluids (except plasmas) the magnetic Reynolds number, Re_m, is much less than unity, which means that the induced magnetic field is very small in comparison with the externally applied magnetic field. Thus, the low-Re_m approximation is valid for the study of this class of turbulent flows (Moreau[1]). With the above assumption, various direct numerical simulations (DNS) have been reported for the study of MHD homogeneous turbulence (e.g., Zikanov and Thess[3]), and turbulent channel and pipe flow (e.g., Branover,[2] Lee and Choi,[4] and Satake, Kunugi, and Smolentsev[5]).

The MHD channel flow with an external magnetic field normal to the walls, usually referred to as the Hartmann flow, has been the subject of various experiments at very high Re numbers, e.g., by Murgatroyd,[6] Reed and Picologlou,[7] and Moresco and Alboussière.[8] These experiments as well as stability analysis, e.g., by Ting and Walker[9] and Krasnov *et al.*,[10] indicate that several properties of the flow depend on the ratio R of the hydrodynamic Reynolds number (Re) to the Hartmann number (Ha). While Ha characterizes the strength of the external magnetic field, the parameter $R=\mathrm{Re}/\mathrm{Ha}$ corresponds to a Reynolds number based on the thickness of the Hartmann layer that develops close to the wall. Although the above studies have used different ducts, the critical value of R for transition to turbulence was consistently found to be in the range $250<R<400$. Thus, even if it is not possible to define a sharp threshold for the transition to turbulence in the Hartmann flow, these values provide a fairly clear indication of the range of R at which the transition is likely to occur under common circumstances.

The present study has several objectives. First, the capability of LES to reproduce the properties of the Hartmann flow close to the transition between laminar and turbulent regimes is investigated. In particular, it is interesting to check that LES confirm the role of the Reynolds number R observed in DNS and in experiments, i.e., the relevant parameter that characterizes the threshold is R, independently of the respective values of Re and Ha. Second, the role of the interaction parameter $N=\mathrm{Ha}^2/\mathrm{Re}$ is also explored. Possible similarities of the flow statistics at constant N are also investigated. It is also explored whether, for turbulent flows at moderate values of the Ha and Re as considered in this study, N might be more relevant than R to characterize the flow, especially for the first order statistics. Finally, the influence of the subgrid-scale model is analyzed, especially as a function of the Hartmann number.

This paper is organized as follows: The governing equa-

[a)]Electronic mail: isarris@ulb.ac.be
[b)]Electronic mail: kassinos@ucy.ac.cy
[c)]Electronic mail: dcarati@ulb.ac.be

 © 2007 American Institute of Physics

This article is copyrighted as indicated in the article. Reuse of AIP content is subject to the terms at: http://scitation.aip.org/termsconditions. Downloaded to IP: 195.130.98.66 On: Tue, 05 May 2015 19:49:17

tions are introduced in Sec. II A and the LES methodology for the Hartmann flow is discussed in Sec. II B. The numerical technique as well as the parameters characterizing the simulation are presented in Sec. III. The results are presented and discussed in Sec. IV and are followed by concluding remarks in Sec. V.

II. GOVERNING EQUATIONS

A. Low magnetic Reynolds number limit

In the limit of low magnetic Reynolds number ($\mathrm{Re}_m \ll 1$), the induced magnetic field is very small when compared to the externally imposed magnetic field $\mathbf{B_0}$ and the electric current $\mathbf{J}$ is given by the Ohm's law,[1]

$$\mathbf{J} = \sigma(-\nabla\Phi + \mathbf{v} \times \mathbf{B_0}), \tag{1}$$

where σ is the electrical conductivity, Φ is the electric potential, ($E=-\nabla\Phi$), E is the electric field, and $\mathbf{v}$ is the velocity field. It is traditional to consider the governing equations for the velocity in terms of nondimensional variables, obtained by introducing a characteristic velocity scale U and a characteristic magnetic field B. In channel flow, the characteristic length scale is usually chosen to be the half-width d. Introducing the dimensionless quantities $\mathbf{b_0}=\mathbf{B_0}/B$, $\mathbf{u}=\mathbf{v}/U$, $\mathbf{j}=\mathbf{J}/(\sigma UB)$, and $\phi=\Phi d/(UB)$, the following equations for an electrically conducting incompressible fluid in the limit of $\mathrm{Re}_m \ll 1$ are obtained:

$$\frac{\partial \mathbf{u}}{\partial t} + (\mathbf{u}\cdot\nabla)\mathbf{u} = -\nabla p + \frac{1}{\mathrm{Re}}\nabla^2\mathbf{u} + N(\mathbf{j}\times\mathbf{b_0}), \tag{2}$$

$$\mathbf{j} = -\nabla\phi + \mathbf{u}\times\mathbf{b_0}, \tag{3}$$

$$\nabla^2\phi = \nabla\cdot(\mathbf{u}\times\mathbf{b_0}) = \mathbf{b_0}\cdot\boldsymbol{\omega}, \tag{4}$$

where Eq. (4) is a consequence of $\nabla\cdot\mathbf{j}=0$ and is obtained by taking the divergence of Eq. (3). Here $\boldsymbol{\omega}=\nabla\times\mathbf{u}$, p the dimensionless pressure and $\mathrm{Re}=Ud/\nu$ is the hydrodynamic Reynolds number, where ν is the kinematic viscosity. Moreover, incompressibility imposes $\nabla\cdot\mathbf{u}=0$.

The traditional choice $B=|\mathbf{B_0}|$ has been adopted for the characteristic magnetic field so that $\mathbf{b_0}$ is a unit vector. In all cases considered in the following, $\mathbf{b_0}$ is normal to the channel walls. The Stuart (or interaction parameter) number, $N=\sigma Bd/\rho U$, is the ratio of the electromagnetic force to the inertial force and it is related to the Hartmann number by $\mathrm{Ha}=\sqrt{\mathrm{Re}N}(=Bd\sqrt{\sigma/\rho\nu})$ where ρ is the density. The characteristic velocity is chosen as the averaged velocity, which is assumed to be directed along the x axis:

$$U = \frac{1}{V}\int d^3\mathbf{r}\, v_x(\mathbf{r}). \tag{5}$$

Such a choice is particularly convenient in our simulations since the flow is driven by imposing a constant mass flux, which amounts to imposing $\partial_t U=0$. Hence, U is constant and its initial value becomes a control parameter that can be used to determine *a priori* the hydrodynamic Reynolds number Re. Equations (2)–(4) are referred to as the low-Re_m MHD equations.

B. Large-eddy simulation of the Hartmann flow

Performing DNS of the Hartmann flow with various values of Re and Ha in order to investigate the possible similarities of the flow properties when either R or N is constant may be extremely demanding in terms of computational resources. Moreover, close to the critical R, the grid has to be fine enough to minimize its influence on the determination of the transition point between turbulent and laminar flow. Thus, even when not fully turbulent, the simulations can be relatively expensive. Boeck *et al.*[11] used DNS to study the effect of increasing R when starting from values close to the threshold. They studied several Ha number cases and reported fully turbulent simulations for $R=450$, and similarity of the turbulent statistics for the same values of R and several combinations of Ha and Re. On the other hand, LES based on subgrid (SGS) models are much faster and have been successfully applied to MHD flows.[12,13] Thus, there is a real motivation to use the LES to investigate the Hartmann flow.

The LES equations for the resolved velocity field $\bar{\mathbf{u}}$ are obtained by applying a spatial filtering to Eqs. (2)–(4):

$$\nabla\cdot\bar{\mathbf{u}} = 0, \tag{6}$$

$$\frac{\partial \bar{u}_i}{\partial t} + \bar{u}_j\frac{\partial \bar{u}_i}{\partial x_j} = -\frac{\partial \bar{p}}{\partial x_i} + \frac{1}{\mathrm{Re}}\nabla^2\bar{u}_i - \frac{\partial \bar{\tau}^{\star}_{ij}}{\partial x_j} + N\{(-\nabla\bar{\phi} + \bar{\mathbf{u}}\times\mathbf{b_0})\times\mathbf{b_0}\}_i, \tag{7}$$

$$\nabla^2\bar{\phi} = \nabla\cdot(\bar{\mathbf{u}}\times\mathbf{b_0}) = \mathbf{b_0}\cdot\bar{\boldsymbol{\omega}}, \tag{8}$$

where $\bar{\tau}^{\star}_{ij}$ is the traceless SGS stress tensor defined by

$$\bar{\tau}^{\star}_{ij} = \bar{\tau}_{ij} - \tfrac{1}{3}\bar{\tau}_{kk}\delta_{ij}, \quad \text{with} \quad \bar{\tau}_{ij} = \overline{u_i u_j} - \bar{u}_i\bar{u}_j. \tag{9}$$

In order to close Eq. (7), $\bar{\tau}^{\star}_{ij}$ has to be expressed only in terms of the resolved velocity. In the case of nonconductive fluids, the most widely used model for $\bar{\tau}^{\star}_{ij}$ is the Smagorinsky model (SM),

$$\bar{\tau}^{\star}_{ij} = -2C_s\bar{\Delta}^2|\bar{S}|\bar{S}_{ij}, \tag{10}$$

where $\bar{S}_{ij}=(\partial_i\bar{u}_j+\partial_j\bar{u}_i)/2$, $|\bar{S}|=\sqrt{2\bar{S}_{ij}\bar{S}_{ij}}$, $\bar{\Delta}$ is the filter width and C_s is the Smagorinsky constant.

However, Shimomura[16] and Kobayashi[13] have already tested several SGS models, including the SM, for the Hartmann flow. Both concluded that the conventional SM is not adequate to predict the turbulent MHD flow, mainly because the value of the Smagorinsky constant is not adapted to MHD turbulence. On the contrary, the dynamic Smagorinsky model (DSM) used by Knaepen and Moin[12] and the coherent structure model (CSM) proposed by Kobayashi[13] are reported to work well. Particularly, Knaepen and Moin[12] have carried out LES of decaying isotropic turbulence under the influence of an external magnetic field using the DSM. Their results have shown that the LES with DSM performs significantly better than the conventional Smagorinsky[14] model (SM), because the Smagorinsky constant automatically decreases while the external magnetic field increases. This property is encouraging since it indicates that the DSM might be able to automatically switch off at the transition

This article is copyrighted as indicated in the article. Reuse of AIP content is subject to the terms at: http://scitation.aip.org/termsconditions. Downloaded to IP: 195.130.98.66 On: Tue, 05 May 2015 19:49:17

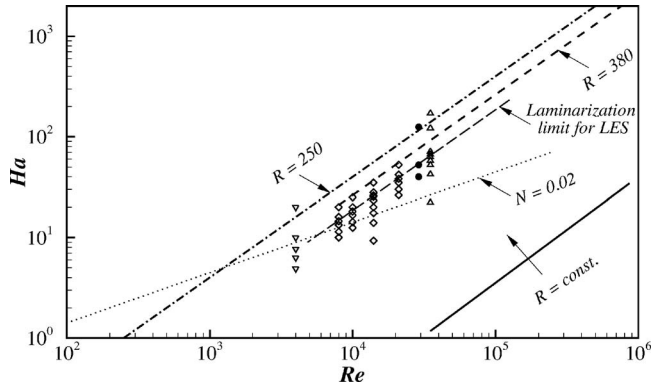

FIG. 1. Re and Ha numbers corresponding to current simulations, ◇. Previous works: ▽, DNS by Lee and Choi (Ref. 4); ●, LES by Shimomura (Ref. 16); △, LES by Kobayashi (Ref. 13) [Re and Ha of the LES of both Shimomura (Ref. 16) and Kobayashi (Ref. 13), and of the DNS of Lee and Choi (Ref. 4), are based on the bulk velocity and the channel width]. The solid line and the arrow indicate the way the present simulations approached the critical value of R.

from turbulent to laminar MHD flow without any special treatment for the magnetic field. This would extend to MHD flow the property shown in various works, e.g., Piomelli and Zang,[15] that the DSM is able to reproduce hydrodynamic transitional wall-bounded flows.

Kobayashi[13] has also shown that both the DSM and the CSM give results in reasonable agreement with the existing experiments of the Hartmann flow by Lykoudis and Brouillette[17] and Reed and Lykoudis.[18] Kobayashi's LES simulations have shown very good agreement with the experimental measurements either for high R numbers (weak magnetic fields), where the flow behaves more hydrodynamically, or for small R numbers, where the strong Lorentz force damps the turbulence. Figure 1 presents in a (Re−Ha) plot the parameter values used by existing DNS and LES works as well as in the present study. In particular, the DNS simulations are laminar at approximately $R=350$ and belong to the regime of $\mathrm{Ha}<20$. Moresco and Alboussière[8] measurements indicate that the flow is laminar for $R=250$ and for $\mathrm{Ha}<20$. Accordingly, laminar solutions for the LES have been reported at approximately $R=550$ by Kobayashi[13] and possibly for slightly higher values of R by Shimomura.[16]

In this study, the dynamic procedure proposed by Germano *et al.*,[19] and, more specifically, the least-square technique suggested by Lilly[20] is systematically used to compute the Smagorinsky constant which can then be expressed as

$$C_s = \frac{\langle \bar{M}_{ij}\bar{L}_{ij}\rangle}{\langle \bar{M}_{ij}\bar{M}_{ij}\rangle}, \tag{11}$$

where $\bar{L}_{ij}$ and $\bar{M}_{ij}$ are given by

$$\bar{L}_{ij} = \widehat{\bar{u}_i\bar{u}_j} - \hat{\bar{u}}_i\hat{\bar{u}}_j, \tag{12}$$

$$\bar{M}_{ij} = 2\bar{\Delta}^2|\bar{S}|\widehat{\bar{S}}_{ij} - 2\hat{\bar{\Delta}}^2|\widehat{\bar{S}}|\hat{\bar{S}}_{ij}. \tag{13}$$

The test-filtered velocity $\hat{\bar{u}}_i$ is calculated using a box filter in physical space. The test-filter width is twice the size of the grid size.

TABLE I. Grid resolution in each direction at the hydrodynamic cases.

Re	Δx^+	$\Delta y^+_{\min}-\Delta y^+_{\max}$	$\Delta z^+_{\max}$
8000	28.2	0.47–10.3	7.05
10000	34.5	0.45–13.3	8.62
14000	46.5	0.44–19.5	11.64
21000	65.0	0.49–28.6	16.25

III. NUMERICAL METHOD

The numerical method used to solve the low-Re_m equations is based on a semi-implicit fractional step method;[21] the diffusion term in Eq. (7) is advanced in time with the Crank-Nicolson method, while the nonlinear, the SGS, and the Lorentz force terms are advanced with a third-order Runge-Kutta (RK3) method. All spatial derivatives are discretized on staggered grids with the second-order central-difference scheme. The Poisson equations for the pseudopressure and the electric potential that are located at the center of each computational cell are solved using a transform method with modified wavenumbers corresponding to the second-order central difference scheme, together with tridiagonal matrix inversion. The time step is automatically computed using a CFL=1 criterion. Once a statistically steady state is reached, the statistics are averaged both in time and in space, in the $x-z$ plane. Based on the streamwise domain size L_x and the bulk velocity U [Eq. (5)], typical integration times are always larger than 200 L_x/U, meaning that, on average, the fluid crosses more than 200 times the computational domain. Moreover, global statistics, like the turbulent kinetic energy, have been checked to be statistically stationary during the period of observation. In this study, the streamwise, wall normal and spanwise direction are, respectively, along the x, y, and z axes.

The simulations are performed using $96\times97\times96$ grid points in a $2\pi\times2\times0.5\,\pi$ computational domain. The choice of the spanwise resolution $(\pi/2)$ has been made for three reasons. First, the optimal wavelength determined by Krasnov *et al.*[10] corresponds to $2\pi/\mathrm{Ha}$ and they used this value as the spanwise size of the computational domain. Hence, for any $\mathrm{Ha}>4$, our computational domain is actually larger. All the runs satisfy this condition, except of course, those with $\mathrm{Ha}=0$, which have been presented mostly to confirm that the code was able to reproduce known results in the hydrodynamic case. The spanwise resolution was also motivated by the same choice $(\pi/2)$ made in existing LES.[13,16] Clearly, choosing the same domain size allows easier comparisons. Finally, it has also been checked that this spanwise domain size is longer than the calculated two-point correlation lengths for all cases studied. The computational grid is stretched in the y-direction using a hyperbolic tangent function and is constant in the other directions. The corresponding grid cell sizes depends on the Reynolds number as presented in Table I for the hydrodynamic cases. Nondimensional units marked by the superscript "+" are defined as $y^+=yu_\tau/\nu$ and $u^+=u/u_\tau$, where

This article is copyrighted as indicated in the article. Reuse of AIP content is subject to the terms at: http://scitation.aip.org/termsconditions. Downloaded to IP: 195.130.98.66 On: Tue, 05 May 2015 19:49:17

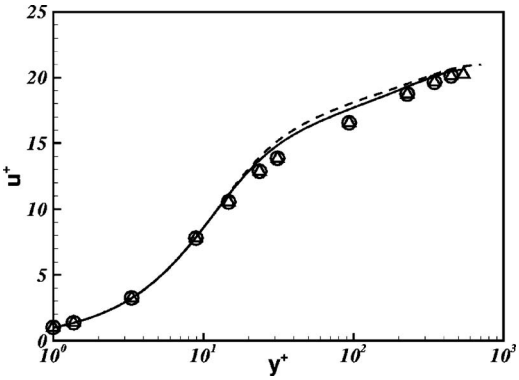

FIG. 2. Comparison against the DNS results of Boeck *et al.* (Ref. 11) for the mean velocity profiles for $R=700$: solid line, present results for Ha$\sim$15; - - -, present results for Ha=20; ○, Boeck *et al.* for Ha=15; Δ, Boeck *et al.* for Ha=20.

$$u_\tau = \sqrt{\frac{\nu}{L_x L_z}\int_0^{L_x} dx \int_0^{L_z} dz \frac{\partial \bar{u}_x}{\partial y}\bigg|_{\text{wall}}} \tag{14}$$

is the friction velocity. Particular care was taken to resolve adequately the Hartmann layers of thickness 1/Ha formed at the channel's walls because of the wall-normal magnetic field. The Hartmann layers in most of the cases are resolved with more than nine grid points, while more than six grid points are used for the higher Hartmann number cases. The present simulations are carried out maintaining a constant mass flow rate in time. The boundary conditions at the non-conducting wall for the resolved quantities are

$$\bar{\mathbf{u}}_{\text{wall}} = 0,\ \bar{j}_y|_{\text{wall}} = -\left.\frac{\partial \bar{\phi}}{\partial y}\right|_{\text{wall}} = 0, \tag{15}$$

where j_y is the wall-normal component of the current density. Periodic boundary conditions are used in the streamwise and spanwise directions. The Hartmann flow, however, requires another condition imposed by the nature of the channel's side walls in the real experiment. Assuming that the channel's side walls constitute an open circuit, the net current through the sidewalls vanishes and the following condition is obtained:

$$\int_0^{L_x} dx \int_{-1}^{1} dy \int_0^{L_z} dz \bar{j}_z = 0. \tag{16}$$

This condition in the presence of a wall-normal external magnetic field implies that the mean spanwise electric field is given by

$$\langle \bar{E}_z \rangle = -\left\langle \frac{\partial \bar{\phi}}{\partial z} \right\rangle = -\frac{1}{2} B_0 \int_{-1}^{1} dy \langle \bar{u}_x \rangle. \tag{17}$$

The code has been first successfully compared against the laminar analytic solution for various Ha numbers (e.g., in Mitchner and Kruger[22]) as well as against the DNS results of Lee and Choi[4] and Boeck *et al.*[11] and the LES results of Kobayashi.[13] In Fig. 2, a comparison between cases 5b and 5c for $R=700$, Ha=15 and 20 against the DNS results from Boeck *et al.*[11] for the mean streamwise velocity u^+ versus y^+ is presented.

TABLE II. Summary of the parameters for the different runs performed.

Case	R	Re	Ha	N
1a	∞	8000	0	0
1b	∞	10000	0	0
1c	∞	14000	0	0
1d	∞	21000	0	0
2a	1500	14000	9.3	0.0062
3a	1000	14000	14	0.014
4a	800	8000	10	0.0125
4b	800	10000	12.5	0.0156
4c	800	14000	17.5	0.0218
4d	800	21000	26.25	0.0328
5a	700	8000	11.42	0.0163
5b	700	10000	14.28	0.0204
5c	700	14000	20	0.0285
5d	700	21000	30	0.0428
6a	600	8000	13.33	0.0222
6b	600	10000	16.66	0.0277
6c	600	14000	23.33	0.0388
6d	600	21000	35	0.0583
7a	550	8000	14.54	0.0264
7b	550	10000	18.18	0.033
7c	550	14000	25.45	0.0462
7d	550	21000	38.18	0.0694
8a	535	14000	26.16	0.0489
9a	500	8000	16	0.032
9b	500	10000	20	0.04
9c	500	14000	28	0.056
9d	500	21000	42	0.084

A number of runs characterized by different Hartmann and Reynolds numbers have been performed (see Table II). Each series of simulations corresponding to the same value of Re (Re=8 000, 11 000, 14 000, and 21 000) is initiated from the hydrodynamic case (Ha=0). Then, Ha is gradually increased in order to determine the value of R that corresponds to the transition to the laminar regime for all four Re numbers. This choice is made to avoid a premature laminarization induced by artificial initial conditions. For the four sets of simulations, the procedure is stopped when a laminar flow is observed.

From the different combinations of Re and Ha numbers presented in Table II, we can also identify groups of similar N numbers. These sets are used in the following to explore the possible role of N in the turbulent regime.

IV. RESULTS AND DISCUSSION

A. LES study of the transition

The averaged turbulent kinetic energy of the resolved velocities versus R is shown for all cases in Fig. 3. As expected, the energy of the fluctuations decreases with R since the Lorentz forces become stronger. For $R<500$ and Re $<14\,000$ the flow is almost laminar for every Re. For Re $=21\,000$ laminarization occurs at higher R, but for Re $<14\,000$, low amplitude fluctuations are still present at R

This article is copyrighted as indicated in the article. Reuse of AIP content is subject to the terms at: http://scitation.aip.org/termsconditions. Downloaded to IP: 195.130.98.66 On: Tue, 05 May 2015 19:49:17

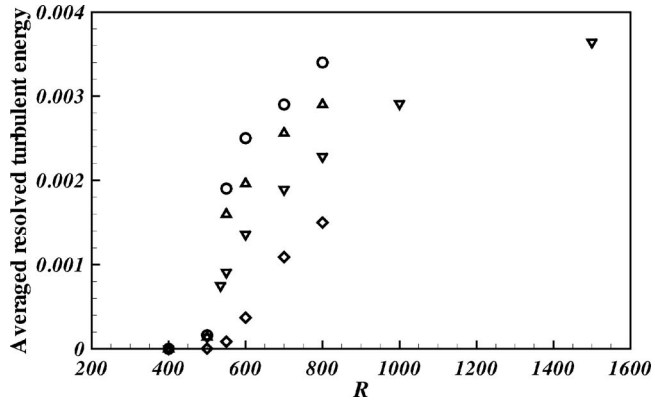

FIG. 3. Averaged resolved turbulent energy vs R: ◇, Re=21000; ∇, Re=14000; △, Re=10000; ○, Re=8000.

=500. The presence of fluctuations with a small turbulent kinetic energy for $R=500$ seems to indicate that the flow has entered a transitional regime (at least in the range Re $<14\,000$).

The decrease of the resolved turbulent kinetic energy, as R is decreased, is also characterized by changes in the flow structure. The flow for high Ha is characterized by the formation of thin Hartmann layers at the walls and by a plateau at the center of the channel. For instance, snapshots of the streamwise velocity in an $x-y$ plane for Re=10 000 at $R=550$ and $R=\infty$ are shown in Fig. 4. In the MHD case at $R=550$, the fluctuations are mostly confined close to the walls and an almost laminar flow exists at the center of the channel, while, using the same scale, the fluctuations are clearly observed in the entire channel in the hydrodynamic case ($R=\infty$).

This behavior can also be observed in Fig. 5 where the mean streamwise velocity profile $\langle \bar{u}_x^+ \rangle$ is plotted in wall units y^+ for different R. Close to the wall all the curves collapse with the wall-law of the hydrodynamic viscous sublayer $[\langle \bar{u}_x^+ \rangle = y^+]$ as already observed in previous studies (see, for example, Ref. 25). This means that very close to the walls no significant deviation from the usual hydrodynamic behavior of the turbulent channel flow is observed. For the hydrodynamic case and the cases of weak magnetic fields ($R \geq 1000$), the mean velocities are similar. However, away

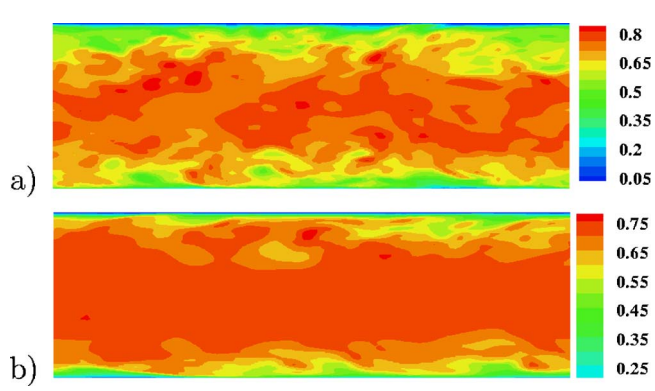

FIG. 4. (Color online) Snapshot of normalized streamwise velocity in an $x-y$ plane for Re=8000: (a) Ha=0 (contour levels: 0:0.067:0.86); (b) $R=550$ (contour levels: 0:0.067:0.78).

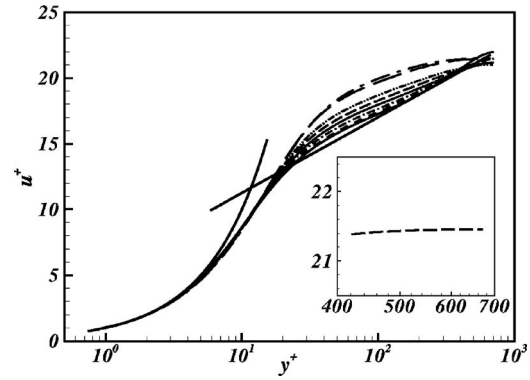

FIG. 5. Mean velocity profiles for Re=14000 as a function of distance from the wall: - - -, $R=1500$; - · -, $R=1000$; · · ·, $R=800$; — — —, $R=700$; – · · –, $R=600$; —- —- —-, $R=550$; — - —, $R=535$. The thin solid line corresponds to the hydrodynamic case and the thick lines to the wall-laws. The internal plot presents the plateau formed in the mean velocity profile for the indicative case $R=700$ in the region $y^+>400$.

from the walls a flattening and a deviation of the usual logarithmic law [i.e., $\langle \bar{u}_x^+ \rangle = 2.5 \ln(y^+) + 5.5$] is observed with the increase of the magnetic field. A logarithmic region seems to be present in most simulations, but its slope tends to decrease with R. Actually, the extension of the logarithmic region seems also to decrease with R and, close to the transition $R \approx 500$, it has almost disappeared.

For $R<1000$ a plateau is observed in the center of the channel as shown in Fig. 5. The formation of the plateau does not necessarily coincide with the laminarization of the flow as can be observed from the root-mean-square resolved velocity fluctuations and from the Reynolds shear stresses shown in Fig. 6. The distribution of the Reynolds shear stresses indicates that the decrease of R damps the flow turbulence, especially at the center of the channel, as expected. In our simulations, the flow remains turbulent even for $R=535$ as Fig. 6 shows. Although the turbulent statistics for $R=535$ and 550 are close, further decrease to $R=500$ results asymptotically in a laminar flow. The critical value of $R \approx 500$ is slightly lower than the value observed in previous LES (Refs. 13 and 16) of the Hartmann flow performed with a lower resolution, but remains higher than the threshold for laminarization experimentally reported by Moresco and Alboussière.[8] It must be noted however that their experiments correspond to much higher hydrodynamic Reynolds and Hartmann numbers than in our simulations, and were performed in a different geometry, a toroidal duct with a square section. Various factors can contribute to the difference between the laminarization threshold found in the present study and the critical Reynolds number for transition reported by Krasnov *et al.*,[10] which they placed in the range $350<R<400$. While one cannot rule out that differences in the numerical methods adopted in the two studies, and the use of a subgrid-scale model in the present LES, could have contributed to this discrepancy, a more likely scenario relates to the transition mechanism active in Hartmann flow. In shear flows with subcritical nonlinear transition, such as Hartmann flow, the Reynolds numbers for transition to turbulence and laminarization do not necessarily coincide. One can speculate that the transition to turbulence was obtained

This article is copyrighted as indicated in the article. Reuse of AIP content is subject to the terms at: http://scitation.aip.org/termsconditions. Downloaded to IP: 195.130.98.66 On: Tue, 05 May 2015 19:49:17

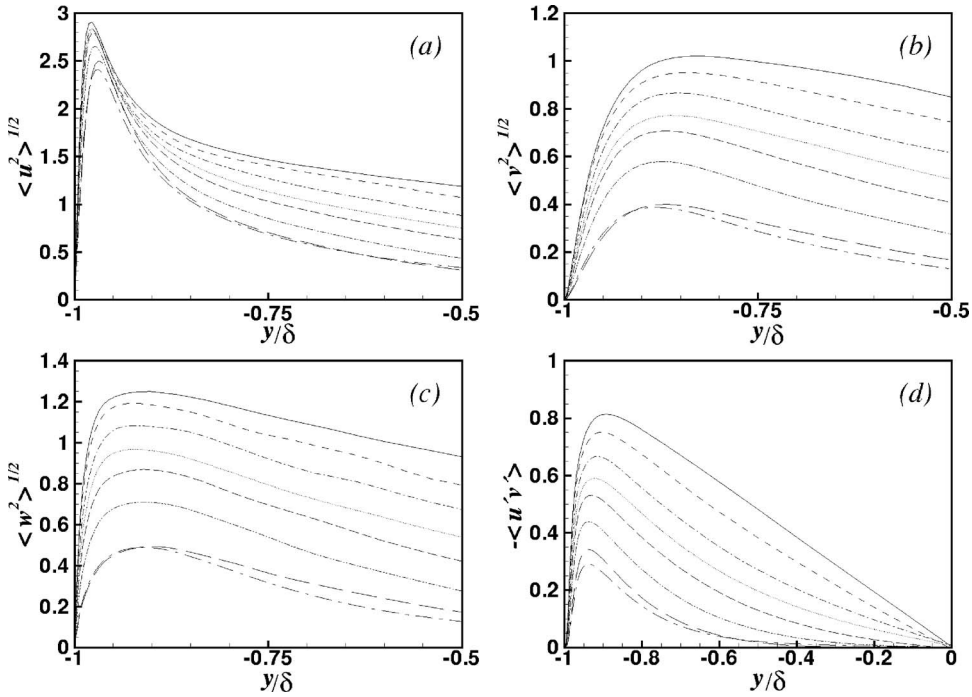

FIG. 6. Root-mean-square resolved velocity fluctuations (a)–(c) and Reynolds shear stress (d) for Re=14000. The rms velocity fluctuations have been normalized with the wall-shear velocity of the hydrodynamic case. The solid line corresponds to the hydrodynamic case. See Fig. 5 for captions.

by Krasnov *et al.* at $350<R<400$ by using special (optimal) initial perturbations. In the absence of such perturbations with sufficiently high amplitude, the laminarization can occur at higher R. In fact, at the end of their paper, Krasnov *et al.* provide evidence that supports this explanation. They showed that starting with 3D perturbations at Re=6600 and Ha=15 (R=440) results in eventual laminarization, albeit after long and eventful evolution that includes growth of streamwise streaks.

B. Similarities of turbulent statistics for constant *R*

The turbulence intensity of the resolved energy reported in Fig. 3 seems to indicate that the statistics of the flow also depend on the hydrodynamic Reynolds number. However, considering the difficulty in accurately determining the transition threshold using numerical simulation, it is remarkable that the four sets of runs corresponding to fairly different Re lead to almost the same critical value of R for the laminarization. Similarities of turbulent statistics for constant R are further studied by considering the runs with R=800 and 600. The ratio between the higher and the lower Ha in each series is approximately 3, and Ha is about 30% higher for R=600.

The mean streamwise velocity profiles are plotted in wall units y^+ for R=800 and 600 in Figs. 7(a) and 7(b). It appears that the results are fairly independent of Re, except for the largest hydrodynamic Reynolds number (cases 4d and 6d).

The rms velocity fluctuations and the Reynolds shear stress for constant R appear to be more sensitive to the increase of Re than the velocity profile. As Figs. 8(a) and 8(b) show for R=800, the higher the Ha, the less intense the turbulence of the Hartmann flow. For Re<21 000, although the amplitudes differ, the shape of the distributions and the positions of their maxima are very close. Note, however, that for the smallest value of Re, the differences in turbulent intensities and Reynolds shear stress are very small.

C. Similarities of turbulent statistics for constant *N*

For the relatively low Re numbers used in the present study, for example much lower than in the experiments by Moresco and Alboussière,[8] the turbulent flow is expected to be quite sensitive to Ha. The turbulent statistics of cases 4 and 6, as presented in Fig. 6, are different than the one for N=0.006 and 0.01, respectively, of Lee and Choi[4] although

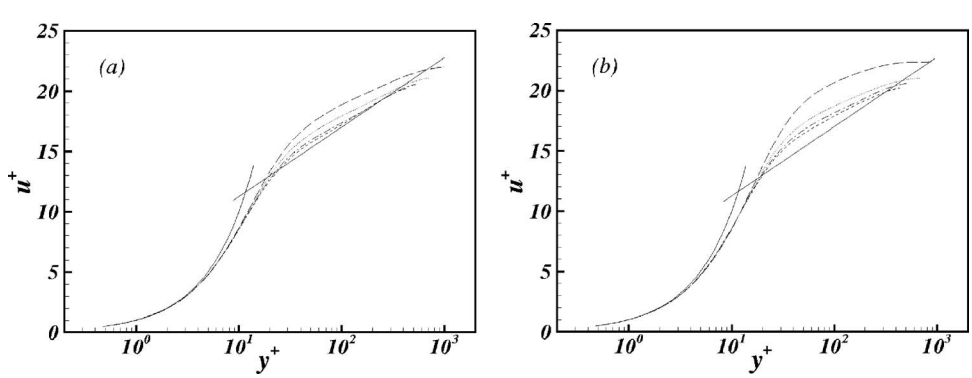

FIG. 7. Mean velocity profiles: (a) R=800: - - -, case 4a; – · –, case 4b; · · ·, case 4c; — —, case 4d, (b) R=600: - - -, case 6a; – · –, case 6b; · · ·, case 6c; — —, case 6d. The solid lines correspond to the hydrodynamic wall-laws.

This article is copyrighted as indicated in the article. Reuse of AIP content is subject to the terms at: http://scitation.aip.org/termsconditions. Downloaded to IP: 195.130.98.66 On: Tue, 05 May 2015 19:49:17

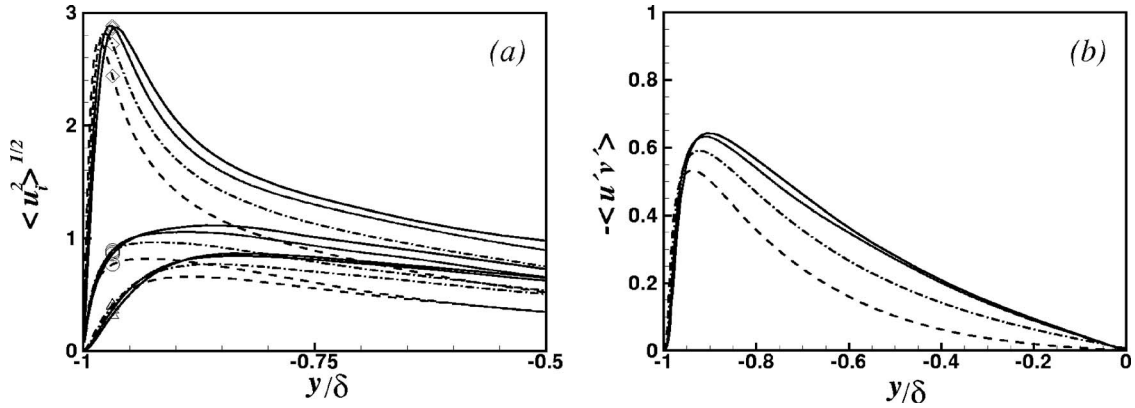

FIG. 8. Root-mean-square resolved velocity fluctuations: ◇, $\langle u^2\rangle^{1/2}$; △, $\langle v^2\rangle^{1/2}$; ○, $\langle w^2\rangle^{1/2}$ (a) and Reynolds shear stress (b) for $R=800$: —, case 4a; · · ·, case 4b; – · –, case 4c; – – –, case 4d. The rms velocity fluctuations have been normalized with the wall-shear velocity of the case Re=14000.

these cases correspond to similar R. In fact, the turbulence appears to be weaker in the case of smaller Re for the same R. A similar conclusion can be reached when compiling the results of Tanahashi *et al.*,[23] Kenjeres *et al.*[24] (especially for the DNS results of Noguchi *et al.* reported therein), Satake *et al.*,[25] and Satake *et al.*[26] Thus, it seems that, for the range of parameters considered here, the results may depend on another parameter than R.

Such a conclusion seemingly contradicts the observations by Boeck *et al.*[11] based on DNS. However, they have been using a definition for the hydrodynamic Reynolds number Re that is based on the centerline velocity of the MHD laminar solution instead of the average velocity U (defined by formula 5) as in Refs. 13, 16, 25, and 26 or the centerline velocity $U_c=3U/4$ of the hydrodynamic laminar solution as in Ref. 4. This difference has the consequence that both the modified Reynolds number R and the interaction parameter N in Ref. 11 have a slightly different meaning. In particular, the four runs at $R=500$ actually correspond to $R=450$, $R=467$, $R=475$, and $R=483$ according to the more traditional definition adopted here.

Nevertheless, it is possible to analyze our result considering that there is another similarity parameter. In particular, we have considered the magnetic interaction parameter N. The comparison of the statistics for constant N was inspired also by MHD homogeneous turbulence studies, see for example, Zikanov and Thess[3] and Schumann.[27] In these studies, results like the energy decay, mean properties and turbulence statistics seem to depend mainly on N even for different Re. Also, the value for N characterizes the flow regime. The same observation can be made here for the averaged turbulent kinetic energy when plotted in Fig. 9 versus N (instead of versus R like in Fig. 3), the resolved turbulent energies for all fully turbulent cases collapse into the same line, independently of the particular values of Re and Ha.

As above, the comparison of the turbulent statistics for constant N is based on the mean velocity and the resolved rms fluctuations. Four series of cases with almost the same interaction parameters ($N\sim0.015$, $N\sim0.02$, $N\sim0.026$ and $N\sim0.032$) have been selected from Table II. The mean streamwise velocity profiles are presented in Fig. 10. Except for minor differences, the mean velocity profiles in all series of cases for constant N collapse on a single curve, much better actually than for constant R. This good match and the reported experience (see, for example, Cabot[28]) that even coarse LES of the channel flow predicts well the first order statistics (fairly close to the DNS) seems to indicate that, at least for the range of the parameters considered here, N can be considered as a similarity parameter.

The situation is however less clear when the resolved rms fluctuations are considered. For instance, considering the cases with $N\sim0.02$ in Fig. 11, it appears that the streamwise component of the root-mean-square velocity fluctuation for cases 6a and 5b matches until $y^+\sim50$, while for the larger Re of case 7b the results are significantly different. The other components of the resolved rms fluctuations are even more sensitive to Re. It must be realized however that the influence of the SGS model is stronger on the high order statistics, especially when Re increases.

D. Influence of the SGS model

As usually in LES studies, it is interesting to compare the eddy viscosity ν_t to the molecular viscosity. In Fig. 12, the profile of ν_t of case 1d is also compared against the results of Cabot[28] for the similar case of $\mathrm{Re}_\tau=1050$. Although certain differences exist between the two cases, the similar ν_t profiles indicate that the present SGS model is performing as expected. When the magnetic field is turned on, the maximal values of ν_t of all cases shown in Fig. 12 are

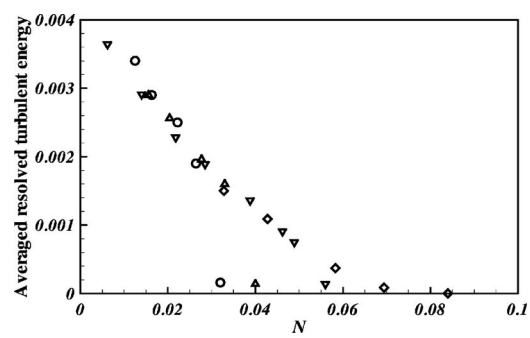

FIG. 9. Averaged resolved turbulent energy vs N: ◇, Re=21000; ∇, Re=14000; △, Re=10000; ○, Re=8000.

This article is copyrighted as indicated in the article. Reuse of AIP content is subject to the terms at: http://scitation.aip.org/termsconditions. Downloaded to IP: 195.130.98.66 On: Tue, 05 May 2015 19:49:17

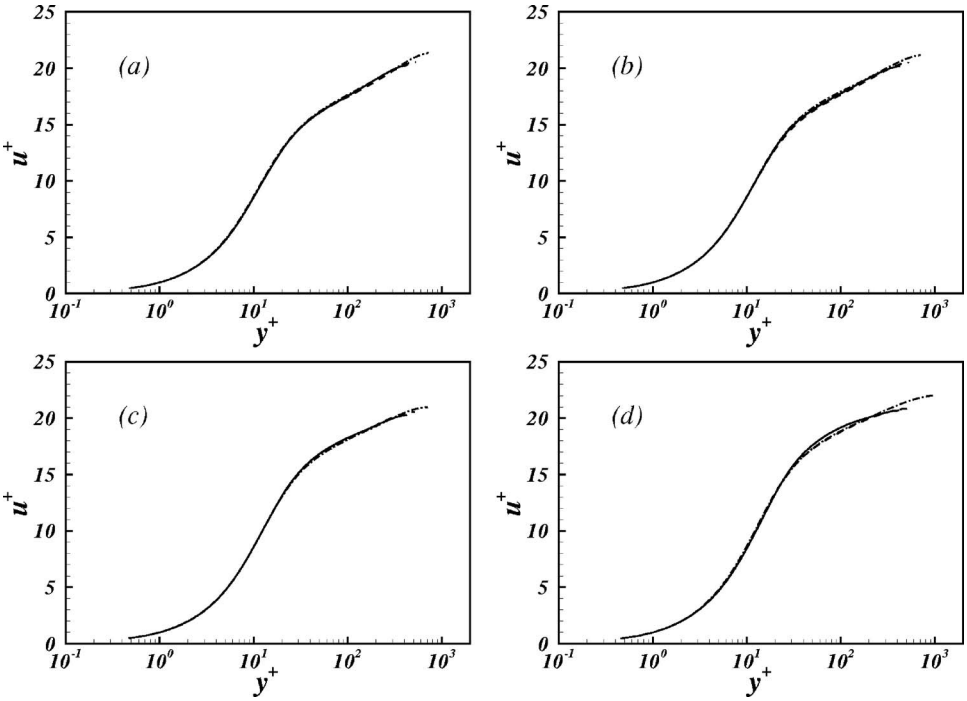

FIG. 10. Mean velocity profiles as a function of distance from the wall: (a) $N\sim0.015$: solid line, case 5c; - - -, case 4b; - · -, case 3a, (b) $N\sim0.02$: solid line, case 6a; - - -, case 5b; - · -, case 4c, (c) $N\sim0.028$: solid line, case 7a; - - -, case 6b; - · -, case 5c, (d) $N\sim0.032$: solid line, case 9a; - - -, case 7b; - · -, case 4d.

reduced. For case 5d that has the same Re as in case 1d, the reduction reaches 40%. This is a direct consequence of the turbulence suppression due to the magnetic field into the SGS model. Thus, the SGS model has less influence for the MHD cases than for Ha=0, because less flow scales have to be modelled. This probably explains why most of our LES results are in reasonable agreement with the DNS results of Boeck *et al.*[11] presented in Fig. 2.

The analysis of the SGS model, keeping constant either R or N, yields the same conclusion. In all cases, as Re increases, the contribution of the SGS model increases because more flow scales have to be modelled. Thus, as in the hydrodynamic case, for increasing Re, the LES results in MHD rely more and more on the SGS model.

It must also be acknowledged that a possible grid dependency may be observed in a LES study. For instance, the threshold R observed by Kobayashi[13] is slightly higher than the value observed here using a finer grid.

V. CONCLUSIONS

The turbulent Hartmann flow has been studied for $8000<\mathrm{Re}<21000$, $9<\mathrm{Ha}<42$, $0<N<0.08$, and $500<R<1500$ using a standard LES procedure based on the dynamic Smagorinsky model. The main objectives were first to investigate the effects of decreasing R for constant Re, and then to examine possible similarities of turbulent statistics for constant R or constant N, but for different Re and Ha numbers.

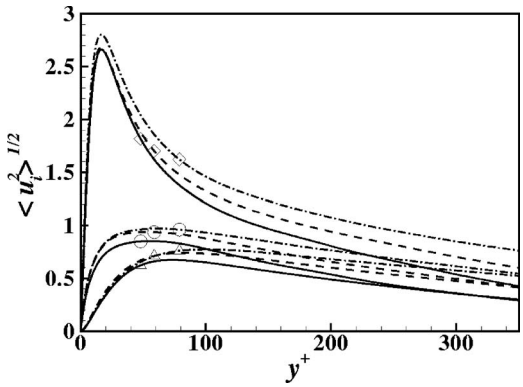

FIG. 11. Root-mean-square resolved velocity fluctuations: ◇, $\langle u^2\rangle^{1/2}$; △, $\langle v^2\rangle^{1/2}$; ○, $\langle w^2\rangle^{1/2}$ for $N=0.02$: solid line, case 6a; - - -, case 5b; - · -, case 4c. The rms velocity fluctuations have been normalized with the wall-shear velocity of each case.

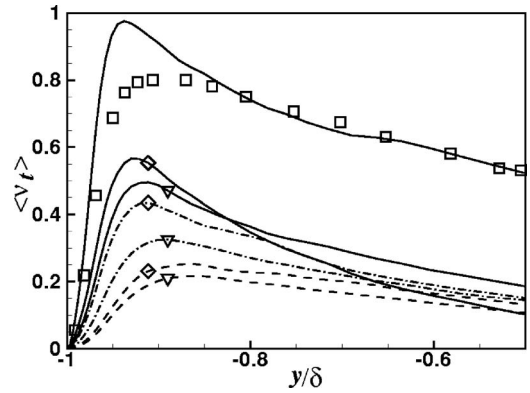

FIG. 12. Mean eddy viscosity (scaled by the molecular value) for constant $R=700$ (lines with ◇: - - -, case 5a; - · -, case 5c; solid line, case 5d) and constant $N\sim0.02$ (lines with ▽: - - -, case 4c; - · -, case 5b; solid line, case 6a). We also provide for comparison, case 1d (solid line) and the results of Cabot (Ref. 28) for the similar $\mathrm{Re}_\tau=1050$, □.

This article is copyrighted as indicated in the article. Reuse of AIP content is subject to the terms at: http://scitation.aip.org/termsconditions. Downloaded to IP: 195.130.98.66 On: Tue, 05 May 2015 19:49:17

As expected, decreasing R has been shown to lead to a relaminarization of the Hartmann flow. Remarkably, despite the fairly low LES resolution used in this study, the laminarization threshold is found to be almost independent of the hydrodynamic Reynolds number, confirming that R is the relevant controlling parameter for the transition between laminar and turbulent MHD channel flow. We note however that the analysis of velocity profiles shows that the similarity parameter could also be taken to be N. For high Ha, the velocity profile exhibits a plateau at the center of the channel and the fluctuations seem to be produced and confined close to the walls. The hydrodynamic viscous sublayer law $\langle \bar{u}_x^+ \rangle = y^+$ is valid for all the studied cases, as already shown in the earlier DNS work of Satake *et al.*,[25] and also repeated by others, i.e. Boeck *et al.*[11] The logarithmic region seems to be quite strongly affected by the value of R. Both its slope and extension decrease with R. As previously mentioned, in the present LES, the logarithmic region almost disappears for small values of R. Remarkably, for moderate hydrodynamic Reynolds numbers, the present LES produce velocity profiles that are almost independent of Re.

These results are very encouraging since many expected features of the Hartmann flows are reproduced by LES using the widely used DSM. Note that this model has not been adapted specifically for MHD, and that exactly the same formalism has been used as in LES of turbulence in nonconductive fluids. This confirms the ability of the dynamic procedure to produce model parameters that are well adapted to the physics of the flows for a wide variety of situations.

ACKNOWLEDGMENTS

The authors would like to acknowledge the contribution of two anonymous referees who made valuable suggestions that helped improve the clarity of the manuscript, especially in connection to the use of N as a similarity parameter and the difference between transition and relaminarization thresholds in shear flows with subcritical nonlinear transition. The authors also gratefully acknowledge financial support from CTR. Stimulating discussions among the MHD group during the 2006 Summer Program influenced the present work significantly. Thomas Boeck, Federico Toschi, Damian Rouson, Chris Dritselis, and Sergey Smolentsev are also acknowledged for their contributions. This work has also been supported by the Fonds National pour la Recherche Scientifique (Belgium, FRFC 2.4542.05), the Fonds Defay, the Communauté Française de Belgique (ARC 02/07-283), the contract of Association EURATOM–Belgian state and the contract of Association EURATOM–Hellenic Republic.

[1] R. Moreau, *Magnetohydrodynamics* (Kluwer, Dordrecht, 1998).
[2] H. Branover, *Magnetohydrodynamic Flow in Ducts* (Halsted, New York, 1978).
[3] O. Zikanov and A. Thess, "Direct numerical simulation of forced MHD turbulence at low magnetic Reynolds number," J. Fluid Mech. **358**, 299 (1998).
[4] D. Lee and H. Choi, "Magnetohydrodynamic turbulent flow in a channel at low magnetic Reynolds number," J. Fluid Mech. **439**, 367 (2001).
[5] S. Satake, T. Kunugi, and S. Smolentsev, "Direct numerical simulations of turbulent pipe flow in a transverse magnetic field," J. Turbul. **3**, 1 (2002).
[6] W. Murgatroyd, "Experiments on magneto-hydrodynamic channel flow," Philos. Mag. **44**, 1348 (1953).
[7] C. B. Reed and B. F. Picologlou, "Side wall flow instabilities in liquid metal MHD flow under blanket relevant conditions," Fusion Technol. **15**, 705 (1989).
[8] P. Moresco and T. Alboussière, "Experimental study of the instability of the Hartmann layer," J. Fluid Mech. **504**, 167 (2004).
[9] A. L. Ting and J. S. Walker, "Linear stability analysis for high-velocity boundary layers in liquid-metal magnetohydrodynamic flows," Int. J. Eng. Sci. **29**, 939 (1991).
[10] D. Krasnov, E. Zienicke, O. Zikanov, T. Boeck, and A. Thess, "Numerical study of the instability of the Hartmann flow," J. Fluid Mech. **504**, 183 (2004).
[11] T. Boeck, D. Krasnov, and E. Zienicke, "Numerical study of turbulent magnetohydrodynamic channel flow," J. Fluid Mech. **572**, 179 (2007).
[12] B. Knaepen and P. Moin, "Large-eddy simulation of conductive flows at low magnetic Reynolds number," Phys. Fluids **16**, 1255 (2004).
[13] H. Kobayashi, "Large eddy simulation of magnetohydrodynamic turbulent channel flows with local subgrid-scale based on coherent structures," Phys. Fluids **18**, 045107 (2006).
[14] J. Smagorinsky, "General circulation experiments with the primitive equations. I. The basic experiment," Mon. Weather Rev. **91**, 99 (1963).
[15] U. Piomelli and T. A. Zang, "Large-eddy simulation of transitional channel flow," Comput. Phys. Commun. **65**, 224 (1991).
[16] Y. Shimomura, "Large eddy simulation of magnetohydrodynamic turbulent channel flows under a uniform magnetic field," Phys. Fluids A **3**, 3098 (1991).
[17] P. S. Lykoudis and E. C. Brouillette, "Magneto-fluid-mechanic channel flow. II. Theory," Phys. Fluids **10**, 1002 (1967).
[18] C. B. Reed and P. S. Lykoudis, "The effect of a transverse magnetic field on shear turbulence," J. Fluid Mech. **89**, 147 (1978).
[19] M. Germano, U. Piomelli, P. Moin, and W. Cabot, "A dynamic subgrid-scale eddy-viscosity model," Phys. Fluids A **3**, 1760 (1991).
[20] D. K. Lilly, "A proposed modification of the Germano subgrid-scale closure method," Phys. Fluids A **4**, 633 (1992).
[21] R. Verzicco and P. Orlandi, "A finite-difference scheme for three-dimensional incompressible flows in cylindrical coordinates," J. Comput. Phys. **123**, 402 (1996).
[22] M. Mitchner and C. H. Kruger, *Partially Ionized Gases* (Wiley, New York, 1973).
[23] M. Tanahashi, D. Fujimura, and T. Miyauchi, "Statistical properties and turbulence structures in MHD channel flow," J. Jpn. Soc. Comp. Fluid Dyn. **b04-3**, 1 (2000).
[24] S. Kenjeres, K. Hanjalic, and D. Bal, "A direct-numerical-simulation-based second-moment closure for turbulent magnetohydrodynamic flows," Phys. Fluids **16**, 1229 (2004).
[25] S. Satake, T. Kunugi, N. Naito, K. Takase, and Y. Ose, "DNS of turbulent channel flow at high Reynolds number under a uniform magnetic field," in Proceedings of the Joint 15th Riga and 6th PAMIR International Conference on Fundamental and Applied MHD (Latvia, 2005, Vol. 1, pp. 175–178.
[26] S. Satake, T. Kunugi, N. Naito, and A. Sagara, "Direct numerical simulation of MHD flow with electrically conducting wall," Fusion Eng. Des. **81**, 367 (2006).
[27] U. Schumann, "Numerical simulation of the transition from three- to two-dimensional turbulence under a uniform magnetic field," J. Fluid Mech. **74**, 31 (1976).
[28] W. Cabot, "Local dynamic subgrid-scale models in channel flow," in *CTR, Annual Research Briefs* (Center for Turbulence Research, Stanford University, Stanford, CA, 1994), pp. 143–159.

This article is copyrighted as indicated in the article. Reuse of AIP content is subject to the terms at: http://scitation.aip.org/termsconditions. Downloaded to IP: 195.130.98.66 On: Tue, 05 May 2015 19:49:17